H.K. Beyer, H.G. Karge, I. Kiricsi and J.B. Nagy (Eds.)
Catalysis by Microporous Materials
Studies in Surface Science and Catalysis, Vol. 94

ESR studies of nitrogen oxides adsorbed on zeolite catalysts: Analysis of motional dynamics

Hidenori Yahiro,[a] Masaru Shiotani,[a] Jack H. Freed,[b] Mikael Lindgren,[c] and Anders Lund[d]

[a]Department of Applied Chemistry, Faculty of Engineering, Hiroshima University, Higashi-Hiroshima 724, Japan

[b]Baker Laboratory of Chemistry, Cornell University, Ithaca, New York 14853, U. S. A.

[c]Chemical Physics Laboratory, IFM Linköping University, S-581 83 Linköping, Sweden

ESR spectra of NO_2 adsorbed on X- and Y-type zeolites were observed in the temperature range 77-346 K. Based upon spectral simulation using a Brownian diffusion model, motional dynamics of NO_2 adsorbed on zeolite surface were analyzed quantitatively. In the case of X-type zeolite, it was found that the ESR spectra below 100 K is near the rigid limit. Above 230 K, the average rotational correlation time decreased from 1.7×10^{-9} (230 K) to 7.5×10^{-10} *sec* (325 K) with increasing temperature and its degree of anisotropy was very close to one (N = 1.25). On the other hand, the temperature-dependent ESR spectra of NO_2 adsorbed on Y-type zeolite were observed to be somewhat different from that for X-type zeolite.

1. INTRODUCTION

Metal- and proton-exchanged zeolites have been recently attracted much attention because of their selective catalytic activity to efficiently reduce nitrogen monoxide (NO) by hydrocarbon in an O_2-rich atmosphere [1]. The formation of nitrogen dioxide (NO_2) from NO and O_2 has been suggested as an important step in the selective reduction [2, 3]. NO_2 is one of rare stable paramagnetic gaseous molecules and has been subjected to electron spin resonance (ESR) studies [4-7]. The ESR parameters and their relation to the electronic structure have been well established [4] and NO_2 can be used as a "*spin probe*" for the study of molecular dynamics at the gas-solid interface by ESR.

More than one decade ago we have reported an ESR study on the molecular motion of NO_2 adsorbed on porous Vycor glass [8,9] and it was found that the NO_2 adsorbed on the Vycor glass and Cu-metal supported on Vycor glass gave strongly temperature-dependence ESR spectra. The present study aimed to further apply our dynamic ESR technique to elucidate motional dynamics of NO_2 adsorbed on various zeolite with different structures. The results can provide fundamental and useful information which are required to develop new active catalyst and to clarify the reaction mechanism.

2. EXPERIMENTAL

X- and Y-type zeolites in a Na^+ form were used as adsorbents. The silica-alumina ratios in the X- and Y-type zeolites measured by the chemical analysis, were 2.5 and 4.9, respectively. NO_2 was obtained commercially and used without further purification. The zeolite samples were activated at 673 K for 4 h under vacuum of 10^{-5} Torr. About 500 Torr of NO_2 was admitted to the zeolite sample at room temperature.

After keeping the sample for several hours adsorbed NO_2 molecules were removed by pumping for 10 minutes at room temperature and subjected to the ESR study. ESR spectra were recorded at X-band with Varian E-12 or Bruker ESP300E spectrometer by employing 100-kHz field modulation. Microwave power was always adjusted so that no saturation occurred. Details of experimental and calculations were described elsewhere [9].

3. RESULTS AND DISCUSSION

3.1. X-type zeolite

Figure 1 shows the temperature-dependent ESR spectra of NO_2 adsorbed on the X-type zeolite. Below 100 K, the ESR spectra of an anisotropic triplet-triplet were observed as shown in Fig. 1(a). The observed ESR line shape was similar to that obtained for NO_2/Vycor system at 4.8 K [9]. The principal values of g and A tensors were evaluated by the ESR spectral simulation method: g_{xx} = 2.0055, g_{yy} = 1.9915, g_{zz} = 2.0015, and A_{xx} =142.6, A_{yy} = 135.2, A_{zz}=195.5 MH_z at 77 K. The x, y, and z components are indicated in the following insert.

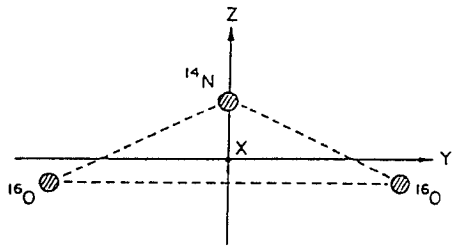

These principal values are in good agreement with those reported for NO_2/Vycor system under rigid limit conditions [9]. The results indicate that spectrum of NO_2 adsorbed on X-type zeolite below 100 K are very close to the rigid limit in the ESR time scale (average rotational correlation time, $\tau_{\bar{R}} > 10^{-6}$ *sec*).

Above 100 K, motional effects on spectrum become pronounced with increasing temperature and, above 230 K, the spectra consist of essentially an isotropic and equally spaced hyperfine triplet, but with different relative intensities. The line shape simulations were carried out by adopting a Brownian rotational diffusion model in order to evaluate the associated (average) rotational correlation time, $\tau_{\bar{R}}$, and its degree of anisotropy, $N = \tau_{R//} / \tau_{R\perp}$ [10, 11]. Here, $\tau_{\bar{R}}$ is defined as $\tau_{\bar{R}} = \sqrt{\tau_{R//} \cdot \tau_{R\perp}} = (6\sqrt{R_{//} \cdot R_{\perp}})^{-1}$ for simple Brownian

diffusion (see ref. 11), where $R_{//}$ and $R_{\perp}$ are the principal values of axial and perpendicular rotational diffusion tensor and $\tau_{R//}$ and $\tau_{R\perp}$ are the corresponding rotational correlation times. The theoretical ESR spectra depicted in Fig. 2 demonstrate how the line shape varied when the molecular axis about which rapid rotational takes place is changed from the z to x or y axis. The spectra in Fig. 2 were calculated by using a set of anisotropic diffusion tensor, $R_{//} = 5.27 \times 10^6$ *sec*$^{-1}$ and $R_{\perp} = 5.27 \times 10^7$ *sec*$^{-1}$ (i.e. $\tau_{\bar{R}} = 1 \times 10^9$ *sec*; $N = 10$) for spectra (b)-(d), while $R_{//} = R_{\perp} = 1.67 \times 10^8$ *sec*$^{-1}$ for isotropic spectrum (a). Comparing the experimental spectra with the theoretical ones, one can find that the ESR line shapes of Fig. 1(f)-(h) in the motional narrowing region ($10^{-8} > \tau_{\bar{R}} > 10^{-11}$ *sec*) are rather close to those of Fig. 2(a) or (c). Spectra (a)-(e) cannot be reproduced by the ESR line shape simulation method since they consist of at least two different spectra.

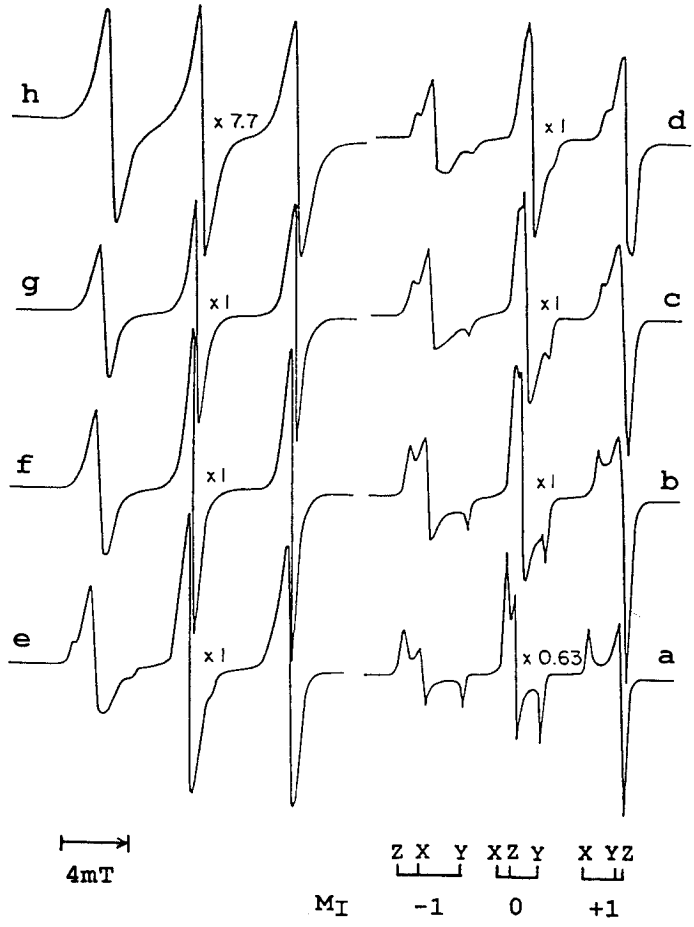

Figure 1. Temperature-dependent ESR line shapes of NO_2 adsorbed on the X-type zeolite with a Na^+ form. Temperature: (a) 93; (b) 164; (c) 185; (d) 200; (e) 212; (f) 250; (g) 293; (h) 346 K.

The peak-peak derivative line width, T_2^{-1}, was well-known to be a function of M_I component ($M_I = \pm 1, 0$ for ^{14}N), in the motional narrowing region.

$$T_2(M_I)^{-1} = A + BM_I + CM_I^2 + \cdots\cdots \quad (1)$$

The coefficients, A, B, and C, were estimated experimentally according to the following equations,

$$A = T_2(0)^{-1} \quad (2)$$

$$B = \tfrac{1}{2} \cdot A \cdot \left(\sqrt{h(0) \cdot h(+1)^{-1}} - \sqrt{h(0) \cdot h(-1)^{-1}} - 1 \right) \quad (3)$$

$$C = \tfrac{1}{2} \cdot A \cdot \left(\sqrt{h(0) \cdot h(+1)^{-1}} - \sqrt{h(0) \cdot h(-1)^{-1}} - 1 \right) \quad (4)$$

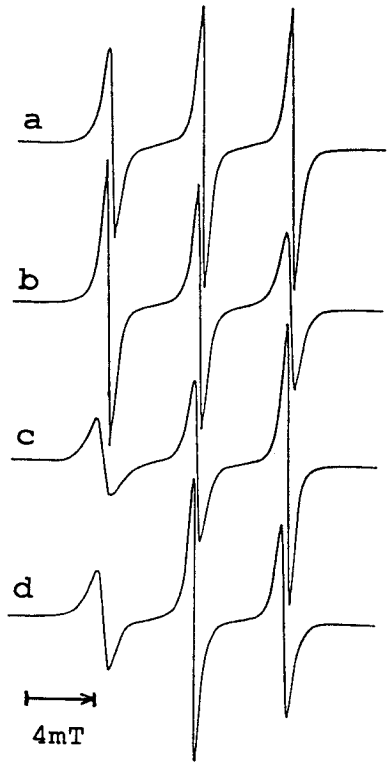

Figure 2. Theoretical spectra of NO_2 anisotropically rotating about its x axis (b), y axis (c), and z axis (d). The spectra were calculated for Brownian rotational diffusion model by using $R_{//} = 5.27 \times 10^6$ *sec*$^{-1}$, $R_{\perp} = 5.27 \times 10^7$ *sec*$^{-1}$ and T_2^{-1}=3.0 G. For isotropic rotation (a), $R_{//} = R_{\perp} = 1.67 \times 10^8$ *sec*$^{-1}$ and T_2^{-1}=3.0 G were used. The rotational diffusion values used through (a) to (d) correspond to a constant value of τ_R=1 x 10^{-9} *sec*. ν, 9.167 GHz.

where $h(M_I)$ stands for peak height at M_I component in ESR spectrum. On the other hand coefficients, B and C, have been theoretically developed by Goldman and coworkers [10]. Employing their expression given in eq. (5) of ref. 10 we evaluated the theoretical values of B and C as a function of $\tau_{\bar{R}}$ and N. Throughout the calculation, we assumed that the axial diffusion axis ($R_{//}$) was coincident with the molecular y-axis, the perpendicular ones ($R_{\perp}$) being with the z and x. The results are summarized in Fig. 3. In this figure, theoretical values indicated with solid and dotted lines. By comparing the experimental values with theoretical ones it was found that $\tau_{\bar{R}}$ decreases from 1.7×10^{-9} (230 K) to 7.5×10^{-10} *sec* (325 K) with increasing temperature and N is very close to one (N = 1.25) in the motional narrowing region. The validity of this analysis was reconfirmed by calculating the ESR line shapes fit very well to the experimental ones at 298 and 346 K using the values of $\tau_{\bar{R}}$ and N given above as shown in Fig. 4.

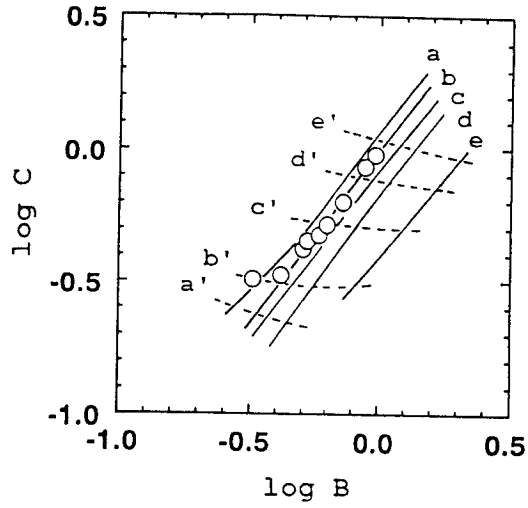

Figure 3. Correlation between coefficients B and C. Open circles stand for the experimental data. Solid and dotted lines are the theoretical values as a function of N and $\tau_{\bar{R}}$. N: (a) 1; (b) 1.25; (c) 1.5; (d) 2; (e) 4. $\tau_{\bar{R}}$: (a') 5×10^{-10}; (b') 7×10^{-10}; (c') 1×10^{-9}; (d') 1.5×10^{-9}; (e') 2×10^{-9} *sec*.

The Arrhenius plots of $\tau_{\bar{R}}$ are given in Fig. 5. From the linear-relationship between $ln\ \tau_{\bar{R}}$ and $T^{-1}(K^{-1})$, the activation energy of 1.4 kcal·mol^{-1} was evaluated for the nearly isotropic rotational diffusion of NO_2 in the X-type zeolite.

3.2. Y-type zeolite

Figure 6 shows the temperature-dependent ESR spectra of NO_2 adsorbed on Y-type zeolite. The line shape change was found different from that for NO_2 adsorbed on X-type zeolite. The x and z components at the M_I = -1 and 0 bands are collapsed into one broad line in the spectrum measured even at 4.8 K, suggesting that the rotational diffusion of NO_2 is axially symmetric about the molecular y axis and high enough to average the A_{zz} and A_{xx} values out. The 4.8 K spectrum can be well simulated by using the following values: $R_{//}$ // y axis= 5×10^8 *sec*$^{-1}$; $R_{\perp}$ //x or z axis = 1×10^6 *sec*$^{-1}$ [9]. The best fit simulations given with dotted lines for a series of temperature-dependent spectra as shown in Fig. 6. Note that $R_{//}$ resulted in almost independent on temperature, while $R_{\perp}$ increased gradually with increasing temperature above 20 K. Thus we observed that the rotational diffusion of NO_2 approaches isotropic motion from anisotropic one with increase in temperature (i.e. N=50 at 23 K; N=7 at 209 K) as seen in

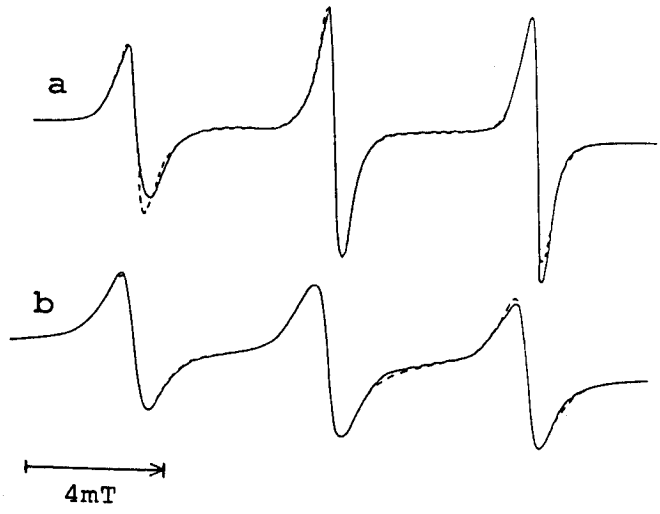

Figure 4. Experimental spectra of NO_2 at (a) 298 and (b) 346 K and best fitting ones shown with dotted lines. The theoretical spectra were calculated by using the values of (a) $\tau_{\bar{R}}$=1 x 10^{-9} *sec* and N = 1.25 and (b) $\tau_{\bar{R}}$=7 x 10^{-10} *sec* and N = 1.

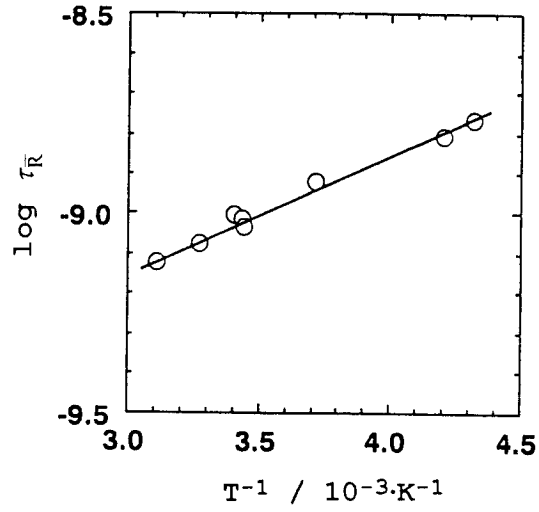

Figure 5. Arrhenius plot of the "average" rotational correlation time, $\tau_{\bar{R}}$, of NO_2 on the X-type zeolite in the motional narrowing region (230 - 325 K). $N = \tau_R / \tau_{R\perp}$=1.25.

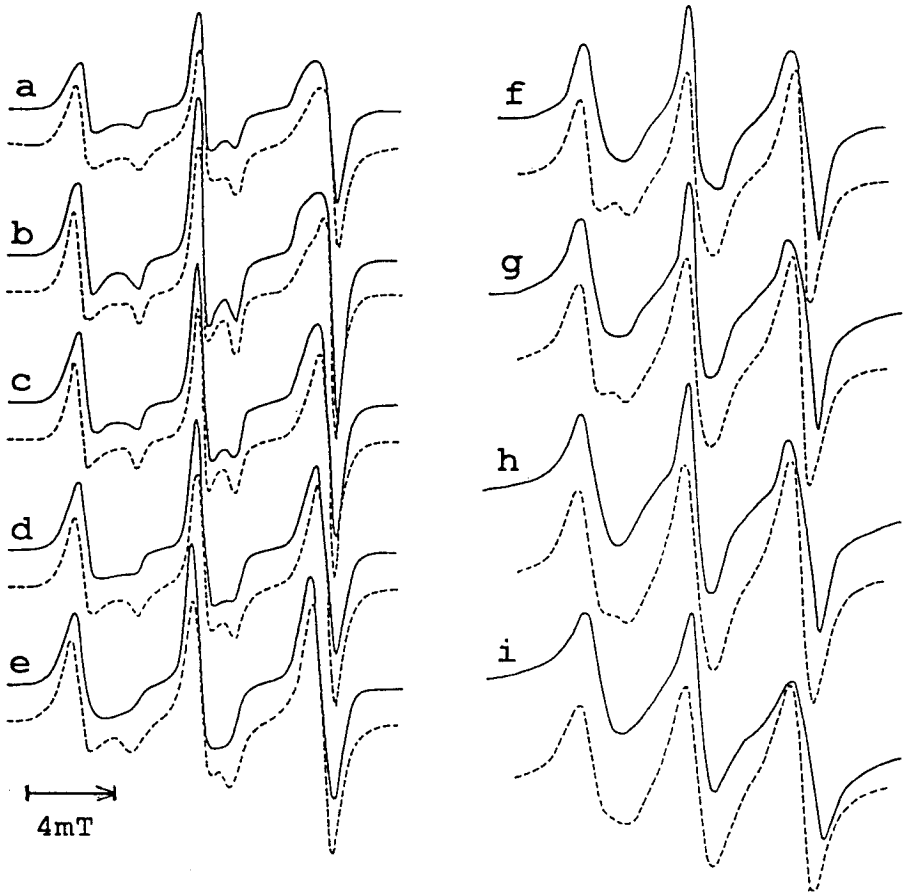

Figure 6. Temperature-dependent ESR line shapes of NO_2 on the Y-type zeolite with a Na^+ form. The dotted lines shows the best-fitting theoretical spectra calculated with Brownian diffusion model. Temperature: (a) 4.8, (b) 15.4, (c) 23.5, (d) 30.5, (e) 39.0, (f) 77, (g) 112, (h) 146, (i) 209 K. For theoretical spectra, (a) $R_{//} = 5 \times 10^7$, $R_{\perp} < 1 \times 10^6$, (b) $R_{//} = 5 \times 10^7$, $R_{\perp} = 1 \times 10^6$, (c) $R_{//} = 7.5 \times 10^7$, $R_{\perp} = 1.5 \times 10^6$, (d) $R_{//} = 1 \times 10^8$, $R_{\perp} = 2.5 \times 10^6$, (e) $R_{//} = 1 \times 10^8$, $R_{\perp} = 5 \times 10^6$, (f)$R_{//} = 1 \times 10^8$, $R_{\perp} = 9.8 \times 10^6$, (g) $R_{//} = 1 \times 10^8$, $R_{\perp} = 1.2 \times 10^7$, (h) $R_{//} = 1 \times 10^8$, $R_{\perp} = 1.2 \times 10^7$, and (i) $R_{//} = 1 \times 10^8$, $R_{\perp} = 1.5 \times 10^7$ *sec.* were used.

Fig. 7. From the linear relation between $ln\ \tau_{R\perp}$ and $T^{-1}(K^{-1})$ in the temperature range 13-209 K, the activation energy of rotational diffusion about the x or z axis was estimated to be 0.1 kcal·mol^{-1}, which is much smaller than that for NO_2/X-type zeolite.

Interestingly it was observed that the line width (T_2^{-1}) increased gradually with increasing temperature. For example, the value of T_2^{-1} was evaluated to be 3.0 G at 23 K and 10.0G at 209 K through the line shape simulation (Fig. 6). This line broadening can not be interpreted by the simple rotational model. The origin of the line broadening will make a subject in forthcoming work.

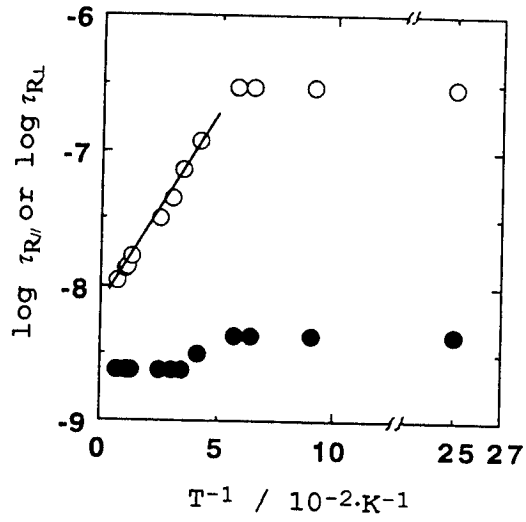

Figure 7. Plots of τ_R (●)and $\tau_{R\perp}$ (○) vs. $T^{-1}(K^{-1})$.

REFERENCES

1. M. Iwamoto and N. Mizuno, *J. Auto Eng.*, **207**, 23 (1993).
2. H. Hamada, Y. Kintaichi, M. Sasaki, and T. Ito, *Appl. Catal.*, **70**, L15 (1991).
3. J. O. Petunchi and W. K. Hall, *Appl. Catal. B*, **2**, 117 (1993).
4. H. Zeldes and R. Livingston, *J. Chem. Phys.*, **35**, 563 (1961).
5. P. W. Atkins, N. Keen, and M. C. Symons, *J. Chem. Soc.*, 2873 (1962).
6. P. H. Kasai, W. Weltner, Jr., and E. B. Wnipple, *J. Chem. Phys.*, **42**, 1120 (1965).
7. J. H. Lunsford, *J. Colloid Interface Sci.*, **26**, 355 (1968).
8. M. Nilges, M. Shiotani, C. T. Yu, G. Barkley, Y. Kera, and J. H. Freed, *J. Chem. Phys.*, **73**, 588 (1980).
9. M. Shiotani and J. H. Freed, *J. Phys. Chem.*, **85**, 3873 (1981).
10. S. A. Goldman, G. V. Bruno, C. F. Polnaszek, and J. H. Freed, *J. Chem. Phys.*, **56**, 716 (1972).
11. J. H. Freed, *"Spin Labelling: Theory and Application"*, L. Berliner, *Ed.*, Academic Press, New York, 1976, vol. 1, Chapter 3.